CCS Chemistry

RESEARCH ARTICLE

Received: Feb. 19, 2022 | Accepted: Mar. 24, 2022 | Published: Apr. 22, 2022

Overcharge to Remove Cathode Passivation Layer for Reviving Failed Li–O_2 Batteries

Kai Chen[1,2], Dong-Yue Yang[1,2], Jin Wang[1], Gang Huang[1,2] & Xin-Bo Zhang[1,2]*

[1]*State Key Laboratory of Rare Earth Resource Utilization, Changchun Institute of Applied Chemistry, Chinese Academy of Sciences, Changchun 130022,* [2]*School of Applied Chemistry and Engineering, University of Science and Technology of China, Hefei 230026*

**Corresponding author: xbzhang@ciac.ac.cn*

Cite this: *CCS Chem*. **2023**, 5, 641–653
DOI: 10.31635/ccschem.022.202201876

Prolonging the lifetime of batteries is a long-term pursuit, and it is also one of the prerequisites for the practical application of batteries. However, this endeavor is challenging for high-energy Li–O_2 batteries due to their poor charge efficiency and cathode passivation-induced by-products accumulation. Here, we demonstrated that overcharging Li–O_2 batteries could facilitate the decomposition of accumulated residue products and revive the cathode; thus, the battery lifespan could be significantly extended. This long battery lifetime not only made full use of the Li anode but also enabled the battery to recycle in a safer way without the risk of firing and explosion. Furthermore, overcharge could be used in Li–O_2 batteries with high mass loading, high rate, and large capacity. This overcharge strategy simplified the cathode regenerating procedures and realized system-level efficient use of battery components, thereby prolonging the life of Li–O_2 batteries to meet the requirements of practical applications.

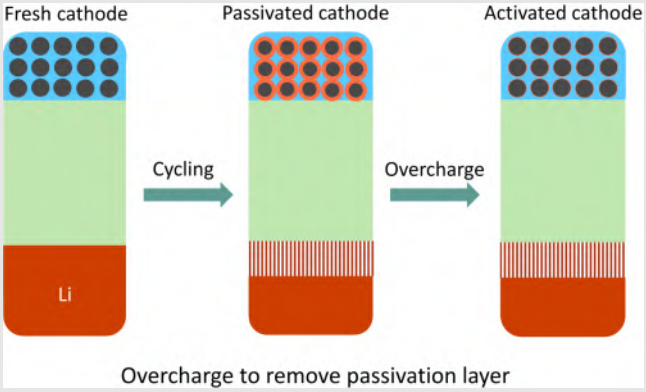

Keywords: **overcharge, Li–O_2 battery, battery life, revive, battery failure mechanism**

Introduction

With a theoretical energy density 10 times higher than current Li-ion batteries (LIBs), Li–O_2 batteries have received intensive research in the past two decades. A typical Li–O_2 battery consists of a Li anode, an organic electrolyte, and a porous cathode and follows the electrochemical reaction of $2Li^+ + O_2 + 2e^- \leftrightarrow Li_2O_2$ with the formation and decomposition of Li_2O_2 during the discharge and charge processes. Though the reaction looks simple, several parasitic reactions occur during battery cycling, making the actual situation of the battery extremely complicated. Especially, the existence of superoxide intermediates, like O_2^- and LiO_2, during battery operation is aggressive toward both the cathodes and electrolytes. Moreover, the discharge product, Li_2O_2, is not completely compatible with the cathode and electrolyte, inducing carbonate films formation at each contact interface.[1] The situation is even worse considering the recently demonstrated singlet oxygen ($^1O_2$), which renders severe electrolyte decomposition.[2] All these parasitic reactions generate hardly decomposed insulating

side products on the cathode. The continuous accumulation of the side products, as cycling goes on, buries the active sites and blocks electron transfer, preventing the proceedings of the electrochemical reactions. Besides the cathode, the Li anode endures grievous corrosion by H_2O and intermediates with the generation of a thick but porous LiOH layer. The degradation of the cathode and anode together limits the lifetime of Li–O_2 batteries, typically <300 cycles, which is far from meeting the requirements of practical applications. Thus, developing methods to prolong the life of Li–O_2 batteries is paramount for bringing Li–O_2 batteries to application.

Traditional methods to extend the life of Li–O_2 batteries include cathode material engineering,[3–5] electrolyte design,[6–11] anode optimization,[12,13] and interphase tuning.[14–17] However, the performance of Li–O_2 batteries is still far from satisfactory. In recent years, numerous conceptual works have been conducted to further boost the life of Li–O_2 batteries, like changing the failed battery with a new cathode and regenerating the degraded cathode by acid wash and high-temperature pulse annealing.[18,19] Although effective, these replacement and regeneration strategies involve tedious battery disassembly and re-assembly procedures, which need to be conducted by professionals. In application scenarios, detailed processes, like battery collecting, transferring, reassembling, and quality checks must be done before usable batteries could be realized, greatly increasing the time and cost, which might not be more economical than assembling new batteries (Figure 1a). Therefore, we investigated whether the cathode could be revived in situ without battery disassembly to aid in extending the life of Li–O_2 batteries while reducing the cost. Since the side products that induce cathode degeneration mainly originate from the poor charge efficiency of Li–O_2 batteries, we considered compensating for the low efficiency by introducing extra charge capacity.

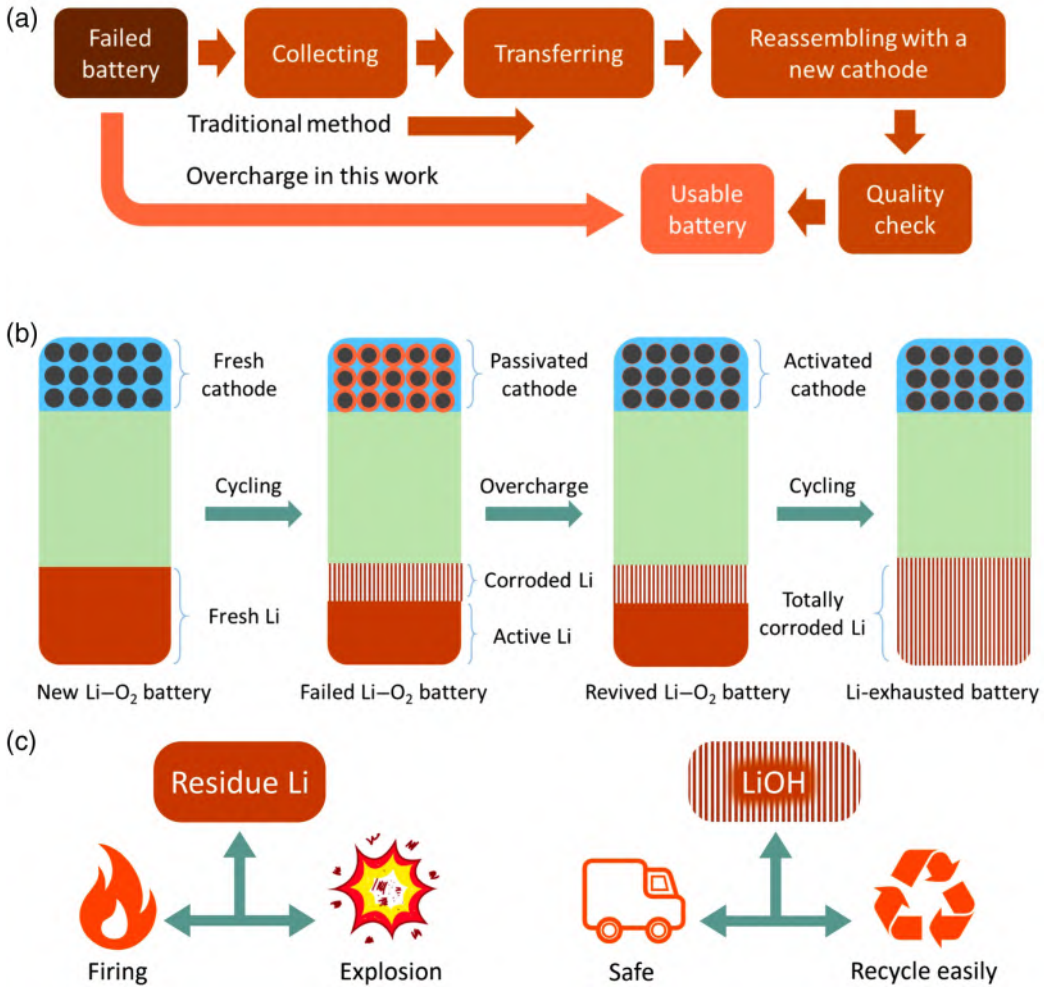

Figure 1 | *Comparison of traditional regenerating method and overcharge method for Li–O_2 batteries. (a) Two kinds of battery regeneration procedures. (b) Schematic illustration of overcharge method. (c) The comparison of properties of residue Li and LiOH in failed Li–O_2 batteries.*

DOI: 10.31635/ccschem.022.202201876
Citation: *CCS Chem.* **2023**, 5, 641–653
Link to VoR: https://doi.org/10.31635/ccschem.022.202201876

For LIBs, overcharge should be avoided due to the consequent negative impacts, including Li deposition on the anode, electrolyte decomposition, cathode structure changes, and capacity fading.[20,21] More seriously, overcharge could lead to gas generation and heat accumulation in the closed system of LIBs.[21,22] Consequently, swelling, rupture, thermal runaway, firing, and even explosion could happen, which pose serious threats to human and device safety. On the contrary, the semi-open nature of the Li–O_2 battery made it possible to withstand the overcharge since the gases generated from side reactions could be liberated, and the flowing gas could eliminate heat and prevent its accumulation. Therefore, the safety of Li–O_2 batteries could be ensured under abusive conditions, including nail penetration, crushing, and high-temperature tests.[23,24] In addition, the semi-open system of Li–O_2 batteries makes electrolyte addition easier than the closed system of LIBs or Li–metal batteries; thus, we could supplement fresh electrolytes to avoid degradation (capacity fading and battery failure) of Li–O_2 batteries.[25] Hence, the unique structure of the Li–O_2 battery enabled it to endure overcharge in a secure manner and prevented the electrolyte from drying up.

Herein, with Li–O_2 battery as an object for detailed research, we demonstrate that overcharging metal–O_2 batteries could prolong their lifetime significantly. The excess amount of Li anode used in the battery makes the culprit of the initial battery failure come from the cathode passivation, induced by continuous side products accumulation and poor charge efficiency. We have identified the main side product is Li_2CO_3 and confirmed its accumulation experimentally. These accumulated side products could be removed through conducting a simple overcharge step, leaving the buried active sites and blocked electron transfer pathways recovered for further proceedings of the electrochemical reactions; thus, the cathode life of Li–O_2 batteries was greatly extended to 1316 cycles. When CO_2 was introduced into the O_2 reaction gas to protect the Li anode, the lifespan was further prolonged, reaching an ultrahigh value of 2714 cycles. Moreover, we checked the application of overcharge in Li–O_2 batteries with high-mass loading cathodes [5 mg cm^{-2} Ru/CNT (Ru/CNT = ruthenium–carbon nanotube)] and still achieved 900 cycles at a high rate of 1 mA cm^{-2} and a capacity of 0.2 mAh cm^{-2}. Furthermore, Li–O_2 batteries with full discharge-charge suffer quick capacity fading; our overcharge strategy could obviously improve capacity retention. Importantly, this overcharge method is also applicable to other metal–O_2 batteries such as Na–O_2 and K–O_2 batteries. The excellent performance improvement enabled by overcharge redefines its functions in batteries by prolonging the life of metal–O_2 batteries in an easy, time-saving, and cost-effective way.

Experimental Methods

Cathode fabrication

CNTs and polyvinylidene difluoride (PVDF) binder material were mixed at a mass ratio of 9:1 in *N*-methyl-2-pyrrolidone to form a homogeneous slurry by a thorough grounding in a mortar. The slurry was then sprayed on carbon paper, followed by overnight drying in a vacuum oven. After this, the dried carbon paper was punched into round pieces (12 mm in diameter) to create cathodes. Several batches of cathodes were prepared with mass loading ranging from 0.1 to 0.3 mg per cathode. The specific capacity was calculated based on the mass of active materials. For the Li–O_2 batteries with a high mass loading (5 mg cm^{-2}) on the cathode (Ru/CNT), the cathode was used as received.

Battery assembly

The batteries were assembled based on ECC-Air models (EL-cell GmbH, Hamburg, Germany) that could flow gas during battery operation. The lithium plate (diameter: 14 mm) was placed at the bottom, followed by the stacking of the glass fiber separator (thickness, 300 μm, diameter, 18 mm) and the prepared cathode (thickness, 200 μm) to obtain a fabricated battery of ~900 μm thickness. The amount of the electrolyte used in the battery was 130 μL. The battery was sealed in the model with a spring. The 900 μm thickness battery had a spring load of 15 N, with a calculated pressure of 1.33×10^5 Pa; the flowing gas was 2 mL/min, and the gas pressure was ~1 atm. After assembly, all prepared batteries were transferred to a thermotank (30 °C) and allowed to rest for at least 3 h to ensure a pure gas environment before cycling.

Operando pressure test

The quantitative pressure test during battery cycling was based on an ECC-Press system (EL-Cell GmbH, Hamburg, Germany) connected with a VMP-300 electrochemical workstation (Biologic, Seyssinet-Pariset, France). Before a test, the free volume of the battery system was determined by Boyle's law. Then the system was purged with pure O_2 to remove the residue gas to ensure a pure O_2 environment. After that, the system was sealed quickly to avoid gas permeation. This test was conducted in a thermotank to minimize temperature fluctuation so that a smooth curve could be achieved.

Characterizations

Before characterization procedures, the cathodes were washed three times with acetonitrile to remove residual electrolytes, while the Li anodes were washed with 1,3-dioxolane (DOL) to remove residual glass fibers and

DOI: 10.31635/ccschem.022.202201876
Citation: *CCS Chem.* **2023**, 5, 641–653
Link to VoR: https://doi.org/10.31635/ccschem.022.202201876

electrolytes on their surface. Both the battery disassembling and electrode washing procedures were conducted in a glove box. After washing, the electrodes were dried in the air-lock chamber and then stored in the glove box. When testing the morphology of the electrodes, they were transferred to a sealed plastic bag to minimize air exposure. A scanning electron microscopy (SEM) test was conducted on a field emission Hitachi S4800 scanning electron microscope (Tokyo, Japan), and the X-ray diffraction (XRD) characterization was performed on a MiniFlex 600 X-ray diffractometer (Rigaku, Tokyo, Japan). Fourier transform infrared (FTIR) measurement was performed on a Nicolet 6700 spectrometer (Waltham, Massachusetts, United States). Battery cycling tests were conducted on a multi-channel battery testing system CT2100A (Wuhan, Hubei, China). Electrochemical impedance spectra (EIS) were performed on a VMP-300 electrochemical workstation.

Results and Discussion

The benefits of overcharge in Li–O_2 batteries

Figure 1b depicts the proposal of cathode regeneration by overcharge. A typical Li–O_2 battery consists of a fresh Li anode and a carbon cathode. During battery cycling, the parasitic reactions and the poor rechargeability result in side products accumulation on the cathode. When the cathode is passivated to some extent, the discharge voltage will plummet to lower than 2.0 V, a sign of battery failure.[4,26] The failed battery is considered useless in most previous investigations. However, at this stage, the anode is not fully utilized because of its excess amount. Disposing of the failed battery leads to safety problems owing to the active nature of the contained lithium and results in resource waste. Therefore, the failed batteries should be recycled to meet the demand for a sustainable and green society. Nevertheless, the traditional procedures for battery recycling are complicated, time-consuming, and costly (Figure 1a), thereby increasing the price of the renewed battery. In contrast, the battery regenerated by a simple overcharge process can prolong its lifespan and maintain a low cost simultaneously. As shown in Figure 1b, after overcharge, the passivation layer on the cathode can be removed, thus, providing free space for the deposition of the following discharge products and enabling the battery to cycle again. This overcharge strategy can be used many times until the exhaustion of active Li, which brings another benefit. If Li residue remains in the battery, risks of firing and explosion exist during reservation and transportation because of its active nature. However, LiOH is much safer and can be easily recycled without considering Li processing (Figure 1c). At this stage, the battery components realize system-level efficient use, and the failed battery is safer; therefore, easy to collect and recycle.

Cathode passivation and overcharge to remove the passivation layer

To confirm the assumptions above, we first verified that the cathode passivation resulted in the initial battery failure rather than the Li anode. As shown in Figure 2a, the newly assembled Li–O_2 battery could run for 100 cycles at a current density of 44.2 μA cm^{-2} and a fixed capacity of 44.2 μAh cm^{-2}. After battery failure (discharge voltage dropped to 2.0 V), the battery was still wetted by the electrolyte. Then the cathode and anode were decoupled and paired with a fresh anode and cathode, respectively, to assemble new batteries and check their viability. From Figure 2b, it is apparent that the battery with the new cathode is able to run for 10 cycles without a drop in the discharge voltage, indicating good cooperation of the new cathode and the remnant of active Li in the old anode. However, even in the first cycle, the battery with the used cathode and fresh Li plate could hardly work, displaying a steep discharge voltage drop to 1.0 V (Figure 2c). As expected, overcharging the battery at 17.7 μA cm^{-2} for 10 h enabled it to deliver a higher discharge voltage in the subsequent cycles even though the voltage decreased gradually. This performance recovery was attributed to the overcharge-induced decomposition of side products on the cathode. Furthermore, the status of the cathode and anode in the initially failed battery was checked using XRD. The XRD patterns of the Li anode showed strong peaks of LiOH, but Li peaks still existed (Figure 2d). The relatively weak signals for Li were due to the upper thick LiOH shielding layer (~131 μm; Supporting Information Figure S1). This meant that only 30% active Li was consumed after the first battery failure, and the residue Li could be a safety threat if not handled properly during battery recycling procedures. For the cathode, the pristine CNTs with a clean surface were fully covered by thick side products (Supporting Information Figure S2), which were in amorphous states since there were no characteristic peaks from Li_2O_2, Li_2CO_3, or other species (Figure 2e). These results unambiguously aided in identifying that the cause of the initial battery failure originated from the cathode passivation, supporting the assumption of reviving the failed battery by following the procedures in Figure 1b.

So the question is, "what causes the side products accumulation on the cathode?" To check the reason, the cathode morphologies were examined after discharge and charge at 0.05 mA for 0.1, 0.2, 0.4, and 0.8 mAh (Supporting Information Figure S3). When the fixed capacity was small (0.1 or 0.2 mAh), the cathode structure could be recovered, with most products removed

DOI: 10.31635/ccschem.022.202201876
Citation: *CCS Chem.* **2023**, 5, 641–653
Link to VoR: https://doi.org/10.31635/ccschem.022.202201876

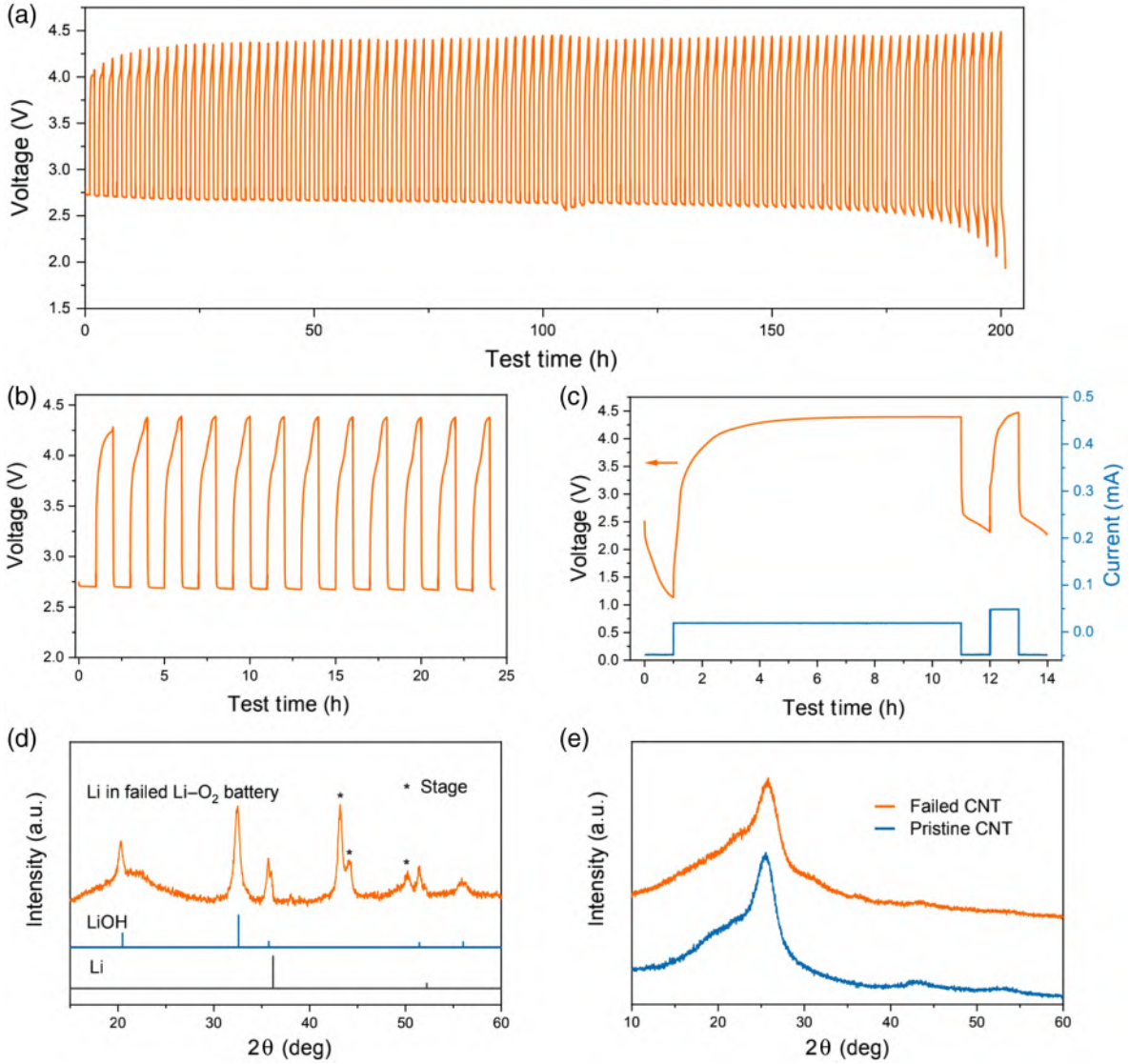

Figure 2 | *Identification of the failure reason for the Li–O_2 battery. (a) Cycling performance of a Li–O_2 battery at 500 mA g^{-1}. (b) The newly assembled battery with the used anode and a new cathode. (c) The newly assembled battery with the used cathode and a new anode. (d) XRD pattern of the anode from the failed battery in (a). (e) XRD patterns of the pristine and failed cathodes from the battery in (a).*

after the subsequent recharge process (Supporting Information Figures S3a and S3b). Even though the undecomposed product was negligible in these small capacities, it was a challenging problem in high-capacity cycling. When the capacity was increased to 0.4 mAh, a passivation layer was observed on the cathode after the charge (Supporting Information Figure S3c). Further, enlarging the capacity to 0.8 mAh, we observed that, except for the passivated film, particle agglomeration emerged (Supporting Information Figure S3d), indicating that the amount of side products increased with the enlargement of the discharge capacity. The poor charge efficiency of Li–O_2 batteries is also reflected in the discharge and charge profiles. In Supporting Information Figure S4a, when the charge capacity reached the discharge value (0.39 mAh), the voltage began to experience a slight increase, followed by a quick rise at 0.45 mAh due to the decomposition of the electrolyte. However, for the battery with a much higher discharge capacity of 2.74 mAh, almost no voltage change occurred when charged at the same capacity (Supporting Information Figure S4b); the sudden death at 2.74 mAh was caused by the low electron and Li^+ conductivity of large-sized Li_2O_2. Even at a 3.22 mAh charge, only a weak voltage increase emerged, implying that the reactions between 2.74 and 3.22 mAh were not significantly different from those before 2.74 mAh. This meant that cycling the battery at capacity-limited mode,

DOI: 10.31635/ccschem.022.202201876
Citation: *CCS Chem.* **2023**, 5, 641–653
Link to VoR: https://doi.org/10.31635/ccschem.022.202201876

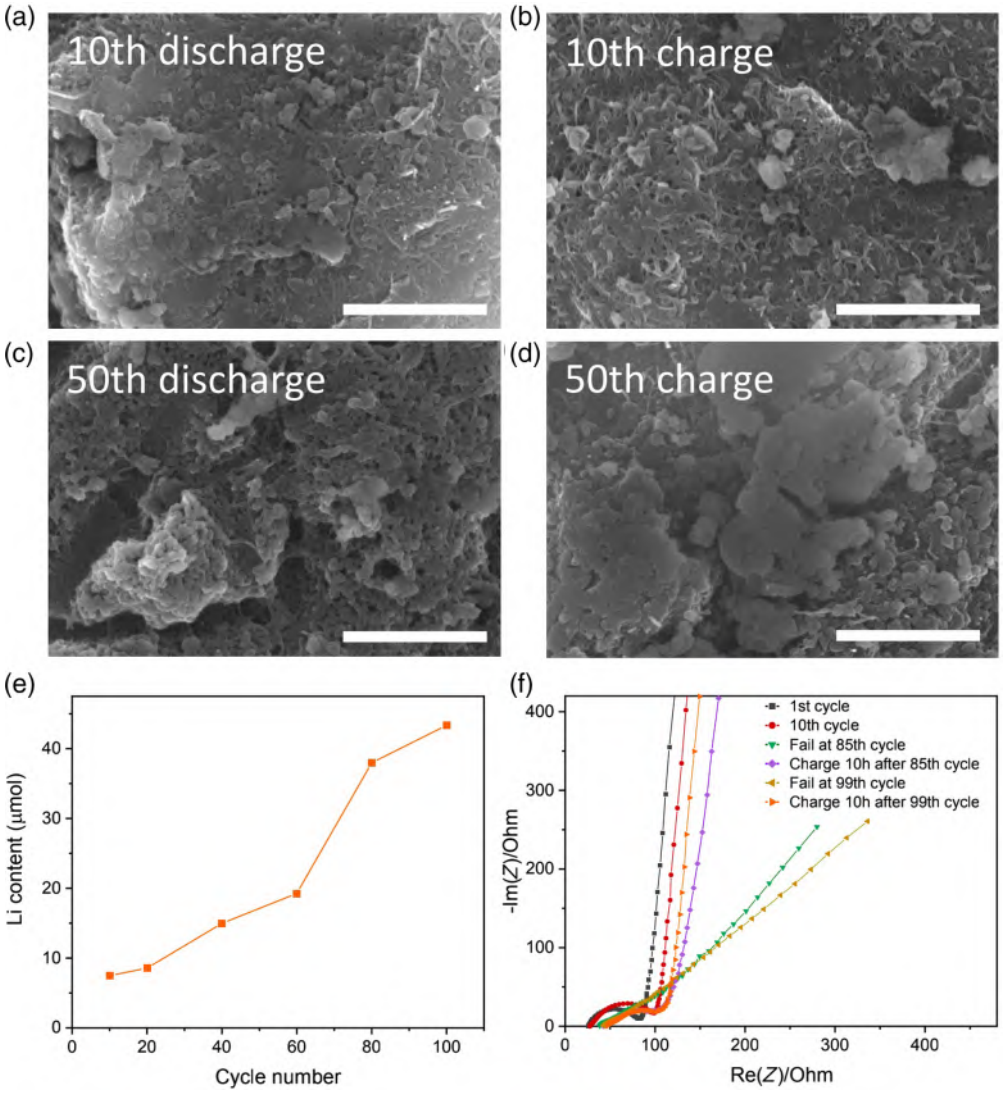

Figure 3 | *Accumulation of discharge products on cathodes. Morphologies of cathodes after (a) 10th discharge, (b) 10th charge, (c) 50th discharge, and (d) 50th charge. Scale bar, 2 μm. (e) Quantification of the products accumulated on cycled cathodes using the acid-base titration method. (f) EIS of Li–O_2 battery at different stages.*

and high discharge depth led to more undecomposed products accumulation on the cathode, and the poor charge efficiency was amplified. As cycling continued, the constant accumulation of the undecomposed product would passivate the cathode completely and cause battery death.

The morphology and composition evolution of the undecomposed product after different cycles were then characterized. After the 10th discharge, the discharge products covered the CNT cathode (Figure 3a), and their composition was confirmed by FTIR spectra with the existence of Li_2O_2 (500–600 cm^{-1}) and Li_2CO_3 (880 and 1400–1520 cm^{-1}) (Supporting Information Figure S5). Although most of the discharge products decomposed and a clear CNT structure was observed during the subsequent charge process (Figure 3b), some undecomposed Li_2O_2 remained, and Li_2CO_3 connected the CNTs. After 50 cycles, more products were deposited on the discharged cathode (Figure 3c), almost exhibiting no decomposition after the charging process (Figure 3d), and was accompanied by peaks from Li_2CO_3, Li_2O_2, HCOOLi, and CH_3COOLi (Supporting Information Figure S5). The results revealed continuous accumulation of these products on the cathode. After confirming the composition of the undecomposed products, we then checked if the reactions were occurring during the overcharge process by monitoring the pressure of the battery to quantify the change of gas. Supporting Information Figure S6a shows the cycling performance of a Li–O_2 battery at 0.1 mA with a fixed capacity of 0.4 mAh. At the 17th cycle, the discharge voltage dropped to 2.0 V, and then the battery was charged for 12 h at 0.1 mA. The

DOI: 10.31635/ccschem.022.202201876
Citation: *CCS Chem.* **2023**, 5, 641–653
Link to VoR: https://doi.org/10.31635/ccschem.022.202201876

pressure change of the battery at this cycle is shown in Supporting Information Figure S6b. The discharge process showed a 2.09 e/gas reaction. Considering O_2 is the main component of the reaction gas; theoretically, 2.0 e/O_2 corresponded to the formation of Li_2O_2 during discharge; thus, the 2.09 e/gas reaction suggested that Li_2O_2 was the dominant discharge product. However, during the overcharge process, the coefficient was much higher than 2.0, reaching 4.01 e/gas. This indicated that generating a gas molecule needed to consume more electrons on average, suggesting that severe side reactions had occurred. These reactions might include the decomposition of previously accumulated products (Li_2CO_3/HCOOLi/CH_3COOLi), generation of aggressive $^1O_2$ and superoxide, and degradation of electrolytes induced by the high voltage (>4.5 V). Importantly, the coefficient value was constant during the entire overcharge process, suggesting similar electrochemical reactions occurred continuously. After overcharge, the battery typically worked with a discharge plateau around 2.6 V (Supporting Information Figure S6b). To identify the gas evolution species, we conducted differential electrochemical mass spectrometry (DEMS) test during the charge process (Supporting Information Figure S7). At the initial 4 h of charge, the dominant evolved gas was O_2 from Li_2O_2 decomposition, while a proportion of CO_2 was also generated at the end of charge (3.5–4 h). However, the amount of CO_2 was very limited compared with the generated O_2, not to mention the O_2 in the entire headspace. Therefore, there was only a slight deviation from the theoretical value during the discharge process. In addition, weak signals with mass to charge ratios (m/z) of 29 and 15 appeared after 1 h of charge and were sustained until the end of overcharge, indicating slight side reactions involving electrolyte decomposition, even though the electrolyte was stable up to 4.6 V (Supporting Information Figure S7c). During the overcharge process (>4 h), the amount of CO_2 increased significantly because of the decomposition of residues (Li_2CO_3/HCOOLi/CH_3COOLi) and the occurrence of other side reactions mentioned above. This confirmed that overcharge could remove the residual products on the cathode to revive it for further cycling.

Since we demonstrated that the initial battery failure was caused by the cathode passivation, we inferred that the battery revival by overcharge could be attributed to the removal of the accumulated products on the cathode, which was visualized, as shown in the Supporting Information Figure S8. After 15 cycles, the cathode was covered by a passivation layer (Supporting Information Figure S8a). It was clear that overcharging the battery for 4 h could remove most of the previously deposited products, leaving only minor aggregates (Supporting Information Figure S8b). When the overcharge time was extended to 8 h, the deposited products were utterly removed (Supporting Information Figure S8c), recovering the cathode to its fresh state, with exposed active sites and ample free space. To quantify the deposited products, we conducted acid-base titration (see Methods section). After 15 cycles, the residues coated on CNT (Supporting Information Figure S8a) were titrated to be 33 μmol. With 4 h of overcharge, the amount of residual products reduced from 33 μmol to 18 μmol, which corresponded to the vanishment of the passivation layer in Supporting Information Figure S8b. In addition, after 4 h of overcharge, only minor particles were detected; thus, another 4 h of overcharge did not reduce the residues totally(from 18 μmol to 16 μmol, Supporting Information Figure S8d); there were still 16 μmol of residues left even though the surface of CNT was clear. We presumed that these residues came from the surface passivation of the CNT structure due to its relatively large surface area (>200 m^2/g). Thanks to the overcharge function of removing the passivation layer, the impedance of the battery decreased with a longer overcharge time (Supporting Information Figure S9).

The above discussions have verified that the gradual increase of the passivation products with prolonged cycling number was due to the negative impact of the poor charge efficiency of Li–O_2 batteries. Hence, we quantified the amount of the accumulated products after different cycles. As shown in Figure 3e, the Li-containing products increased as the cycling continued, although the increasing trend was not linear. This confirmed the accumulation of residual products on the cathodes during cycling. The EIS in Figure 3f also showed a higher impedance at the 10th cycle than at the 1st cycle. When the battery failed at the 85th cycle, the impedance increased further and was much higher than the initial value owing to the significant amount of undecomposed products accumulation on the cathode. However, after overcharging for 10 h, the impedance recovered to a normal value, enabling the battery to continue cycling for another 14 cycles. Notably, the strategy of reviving the battery by overcharge could be repeated several times until the active Li was used up.

Overcharge to realize long-life Li–O_2 batteries

Following the demonstration that overcharge could indeed remove undecomposed products on the cathode and revive the battery for further cycling, the long cycling performance of Li–O_2 battery with overcharge deserved testing to validate its advantages fully. As shown in Figures 4a and 4b, the Li–O_2 battery failed after 180 cycles, and a 4-h overcharge enabled it to work normally for extra 10 cycles before the voltage dropped to 2 V at 387 h (Figure 4b). Every time the battery failed, an overcharge was conducted, and the process could be repeated many times. It is worth mentioning that for a Li–O_2 battery, the electrolyte was constantly consumed during the cycling process because of side reactions and

DOI: 10.31635/ccschem.022.202201876
Citation: *CCS Chem.* **2023**, 5, 641–653
Link to VoR: https://doi.org/10.31635/ccschem.022.202201876

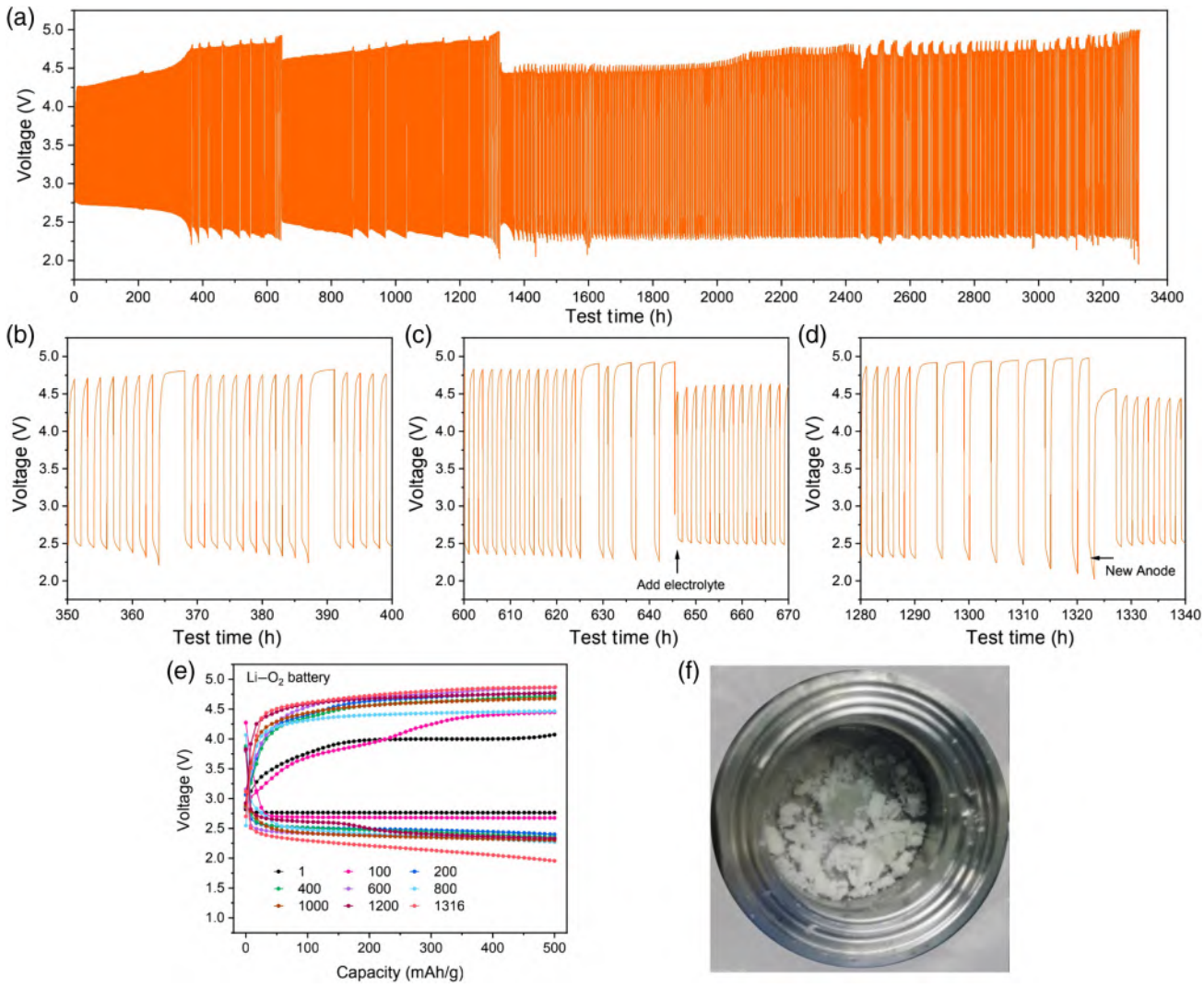

Figure 4 | *The effects of overcharge on the Li–O_2 battery. (a) Cycling performance of a Li–O_2 battery revived with overcharge (1316 cycles). (b–d) The enlargements of the profile in (a). (e) Selected cycles from (a). (f) A digital image of the exhaustive Li anode after cycling. The current density is 500 mA g^{-1}, and the capacity is 500 mAh g^{-1}.*

volatilization. Adding electrolyte to the battery could no doubt help extend the battery life as well, and this was possible due to the semi-open structure of the Li–O_2 battery that could be achieved readily without the requirement of battery disassembly like LIBs. Therefore, when an overcharge could not revive a battery, about 150 μL of electrolyte was added (Figure 4c) to check the cathode limit after overcharging for regeneration, which is not common in practical scenarios. After resting 2 h for electrolyte wetting, the battery could run again, and the discharge voltage plateau recovered. In the following cycles, 4-h-overcharge was adopted when the battery failed. After 624 cycles (1320 h), the anode was exhausted (Figure 4f), then a new anode was utilized to couple with the original cathode to reassemble the battery, with added electrolyte to wet the anode. Surprisingly, this battery could keep running, sustaining a stable discharge plateau (Figure 4d). The overcharge, electrolyte addition (twice), together with the refreshment of the Li anode finally enabled the Li–O_2 battery to deliver a long life of 1316 cycles (Figure 4e). Knowing that the cathode could be regenerated continuously by overcharge and easy addition of electrolyte to the battery, the life of the Li–O_2 battery could only be limited by the durability of the Li anode (Figure 4a). Hence, we envisioned that adopting Li protection strategies could further improve the battery performance and avoid Li anode replacement. In our previous work, we verified that CO_2 could stabilize the Li–O_2 batteries by forming a protective Li_2CO_3 layer on the Li anode and capturing superoxide radical ($O_2^{-\bullet}$).[27] In terms of the benefits of CO_2, a Li–O_2/CO_2 battery was constructed to take full

DOI: 10.31635/ccschem.022.202201876
Citation: *CCS Chem.* **2023**, 5, 641–653
Link to VoR: https://doi.org/10.31635/ccschem.022.202201876

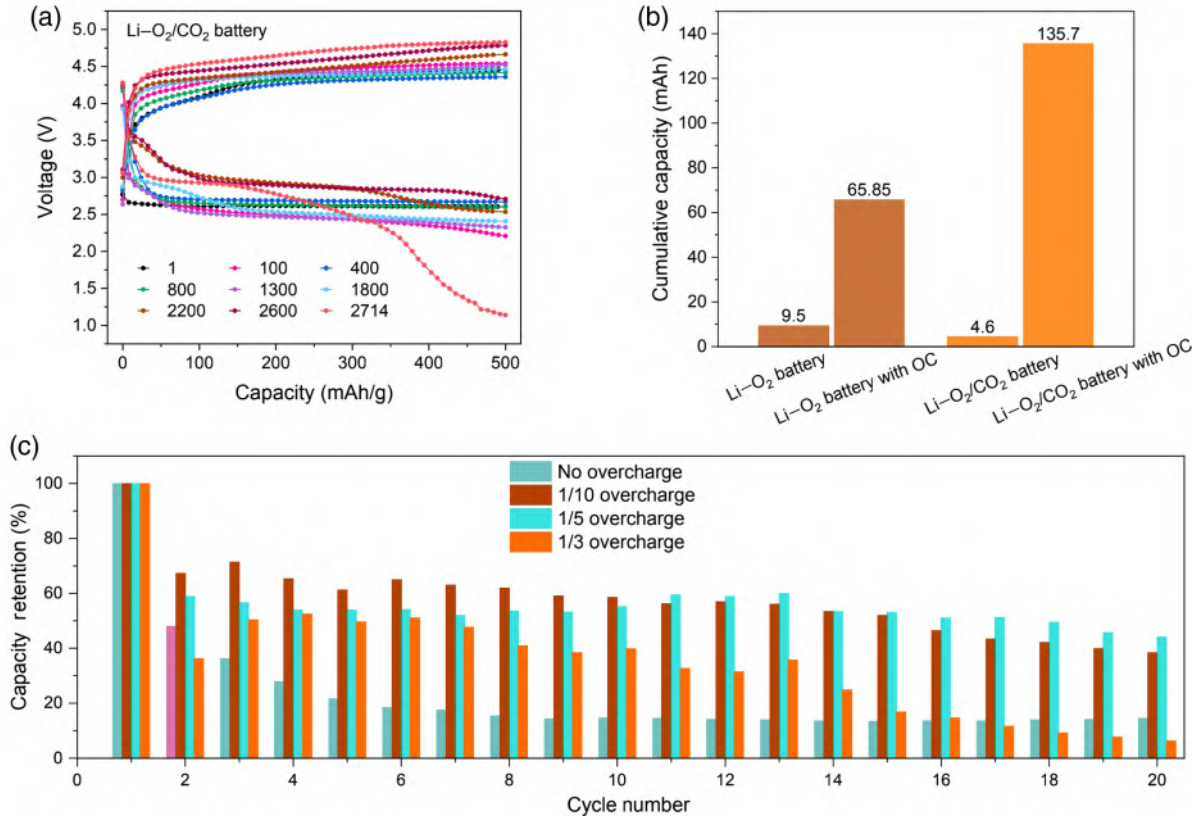

Figure 5 | *Battery performance characterization. (a) Cycling performance of the Li–O_2/CO_2 battery at 500 mA g^{-1} and 500 mAh g^{-1}, revived with overcharge after battery failure. (b) Cumulative capacities of Li–O_2 and Li–O_2/CO_2 batteries with and without overcharge (OC). (c) Capacity retention of Li–O_2 batteries in the first 20 cycles with different overcharge ratios.*

advantage of the cathode and anode and further extend the battery's life (Supporting Information Figure S10a). The Li–O_2/CO_2 battery first failed after 92 cycles, followed by a 4-h overcharge, after which it worked normally (Supporting Information Figure S10b). As expected, the integration of overcharge and two times electrolyte addition eventually made the Li–O_2/CO_2 battery realize a record-high lifetime, reaching 2714 cycles (Supporting Information Figure S10 and Figure 5a, ~270 days) without replacing the Li anode. The stabilization effect of CO_2 on Li anode was proved by the clean surface after 626 cycles (Supporting Information Figure S11a). However, the ultimate failure of the Li–O_2/CO_2 battery resulted from the Li anode pulverization and exhaustion because of the ultra-long cycling (Supporting Information Figure S11b); thus, we expected the battery could live longer if a better anode protection strategy could be developed in the future.

The cumulative capacities of the Li–O_2 and Li–O_2/CO_2 batteries were 9.5 and 4.6 mAh, respectively, before the first failure. With overcharge, the cumulative capacities were enhanced to 65.85 mAh for the Li–O_2 battery and 135.7 mAh for Li–O_2/CO_2 battery (Figure 5b). This great improvement was ascribed to the effective revival of the degraded cathode by overcharge. Even though the cumulative capacity was improved dramatically with the help of overcharge, the Li efficiency was still too low, which is also a long-neglected problem in Li–O_2 batteries. In typical Li–O_2 batteries, the Li anode is excessive because the semi-open structure causes reactive O_2, CO_2, and H_2O to consume Li. In our systems, the capacity of the Li plate is 158 mAh, suggesting that the efficiencies for the overcharged Li–O_2 and Li–O_2/CO_2 batteries are 20.8% (based on two plates) and 85.9%, respectively. Efforts to improve Li efficiency and cycling stability of Li–O_2 batteries based on low excess Li were essential to reduce cost and increase energy density. Furthermore, we conducted battery cycling tests at full discharge state (discharge to 2.0 V) and checked the capacity retention by overcharging the battery with an additional 1/10, 1/5, and 1/3 capacity (Supporting Information Figure S12). We observed that the battery without overcharge displayed the poorest capacity retention: only ~20% of the initial capacity could be delivered at the 6th cycle (Figure 5c). For the overcharged batteries, the two with 1/10 and 1/5 overcharge attained a comparable capacity

DOI: 10.31635/ccschem.022.202201876
Citation: *CCS Chem.* **2023**, 5, 641–653
Link to VoR: https://doi.org/10.31635/ccschem.022.202201876

retention rate of about 40% after 20 cycles, while only 14.56% and 6.35% remained in the batteries without overcharge and with 1/3 overcharge. The total capacities of the four batteries delivered in the first 20 cycles were 4.54 (no overcharge), 11.60 (1/10 overcharge), 11.19 (1/5 overcharge), and 6.99 (1/3 overcharge) times as much as their first discharge capacities (Supporting Information Figure S12e), respectively, meaning that the higher degree of overcharge cannot always bring better capacity retention, it should be rationally controlled.

We further checked whether our overcharge strategy could prolong the life of Li–O_2 batteries with a redox mediator. A Li–O_2 battery with 50 mM LiI in the electrolyte was tested at 200 mA g^{-1} with a capacity of 2000 mAh g^{-1}. As shown in Supporting Information Figure S13, just after 15 cycles, the battery failed. After overcharge, the battery could run for another 5 cycles. After overcharging again, the battery ran for more than 56 cycles. The battery achieved a final life of 88 cycles, ~5 times longer than the initial 15 cycles.

The general applicability of overcharge in metal–O_2 batteries

We acknowledged that the development of Li–air batteries is still far from extensive application because many challenges still exist, including the small active material loading on the cathode. In the future, mass loading increase from sub-milligram to milligram level should be considered to boost energy density while maintaining a long cycling life. To prove the potential of overcharge in a real-world application, Li–O_2 batteries with 5 mg Ru/CNT@carbon papers (1 cm^2) as cathodes were tested without anode replacement or electrolyte addition. After battery failure, the surface of Ru/CNT was covered by residue products (Figure 6a); these residues could be decomposed when conducting an overcharge process, which left uncovered CNT structures (Figure 6b), proving that overcharge could remove the excessive products even in the cathode with such a high mass loading. Then the battery cycling performance was checked under different conditions. Figure 6c exhibits the performance at 1 mA cm^{-2} with a fixed capacity of 0.2 mAh cm^{-2}. This battery failed after a short time (24 cycles); after subsequently repeated overcharge to prolong its lifespan, 900 cycles were achieved at a high current density of 1 mA cm^{-2}, which is rarely used in previous reports, considering the trade-off between current density, cycling life, sluggish ORR reaction, and Li dissolution in tetraglyme. In addition, high current density could lead to the formation of quasi-amorphous thin Li_2O_2 films that cover the cathode surface to prevent further discharge of the battery. Therefore, with a cycling capacity of 0.2 mAh cm^{-2}, the battery achieved an unprecedented lifespan at such a high current. Furthermore, batteries with higher capacities (0.5 and 1 mAh cm^{-2}) are presented in Supporting Information Figure S14, showing batteries cycled at 0.5 mA cm^{-2} and 0.5 mAh cm^{-2}, and 0.2 mA cm^{-2} and 1 mAh cm^{-2} realized 325 cycles and 91 cycles, respectively, far exceeding those without the overcharge process. Given that high mass loading is less used in Li–O_2 batteries, a list has been made to emphasize the further benefits that overcharge brings to the battery performance (Supporting Information Table S1). Moreover, we compared the full discharge-charge cycling performance of batteries with 2.0 V as the cut-off voltage at 0.25 mA cm^{-2}. As shown in Figures 6d–6f, the capacity retention of the battery with 10% overcharge could sustain above 50% after 12 cycles. However, the capacity of the battery without overcharge faded quickly, with only ~10% capacity left after 5 cycles. This noticeable difference was attributed to the overcharge-induced passivation layer removal, which highlighted the effective role of overcharge in capacity retention.

We note that no extra electrolytes were added or Li replacement during the long cycling, and even the cathode loading increased to 5 mg cm^{-2}, the amount of electrolyte added during battery assembly was kept at 130 μL despite the thicker cathode (419 μm). It should also be mentioned that there was an abnormal phenomenon at the later stage of the cycling: each overcharge could enable longer cycles (13,500–22,000 min in Figure 6c). As we know, besides solvent evaporation, the decompositions of electrolyte and Li_2O_2 compete and proceed simultaneously during charge. This could cause limited amounts of liquid electrolyte to transform into the stable solid-state electrolyte (SSE), and thus, the decomposition of Li_2O_2 could prevail. Accordingly, the accumulation of side products is alleviated, and the battery life is extended naturally. To confirm this conjecture, the failed battery was characterized. During batteries disassembly, the electrolyte was totally drained with the emergence of powders on the cathode and the separator (Supporting Information Figure S15a). A subsequent check on the interface between the cathode and separator revealed that they were in close contact after battery disassembly. In Supporting Information Figure S15b, the cross-section image reveals that the gap between the glass fiber separator and cathode is only 50 μm at a relaxed state, which could be pressed tightly when applying pressure. After being detached, the contact interface between the cathode and separator was checked by SEM. Both surfaces were found to hold solid electrolytes closely (Supporting Information Figures S15c and S15d), possibly to enable a dense connection of the cathode and separator to transfer Li^+. Thus, the surfaces of the cathode and separator toward the interface side were characterized by Raman spectroscopy (Supporting Information Figure S15e). The strong signals at 762, 1044, 1231, and 1085 cm^{-1} indicated the existence of $LiCF_3SO_3$, Li_2CO_3, and a trace amount of the aprotic solvent tetraethylene glycol dimethyl ether (TEGDME; 1434–1489 cm^{-1}) trapped in the solid-state

DOI: 10.31635/ccschem.022.202201876
Citation: *CCS Chem.* **2023**, 5, 641–653
Link to VoR: https://doi.org/10.31635/ccschem.022.202201876

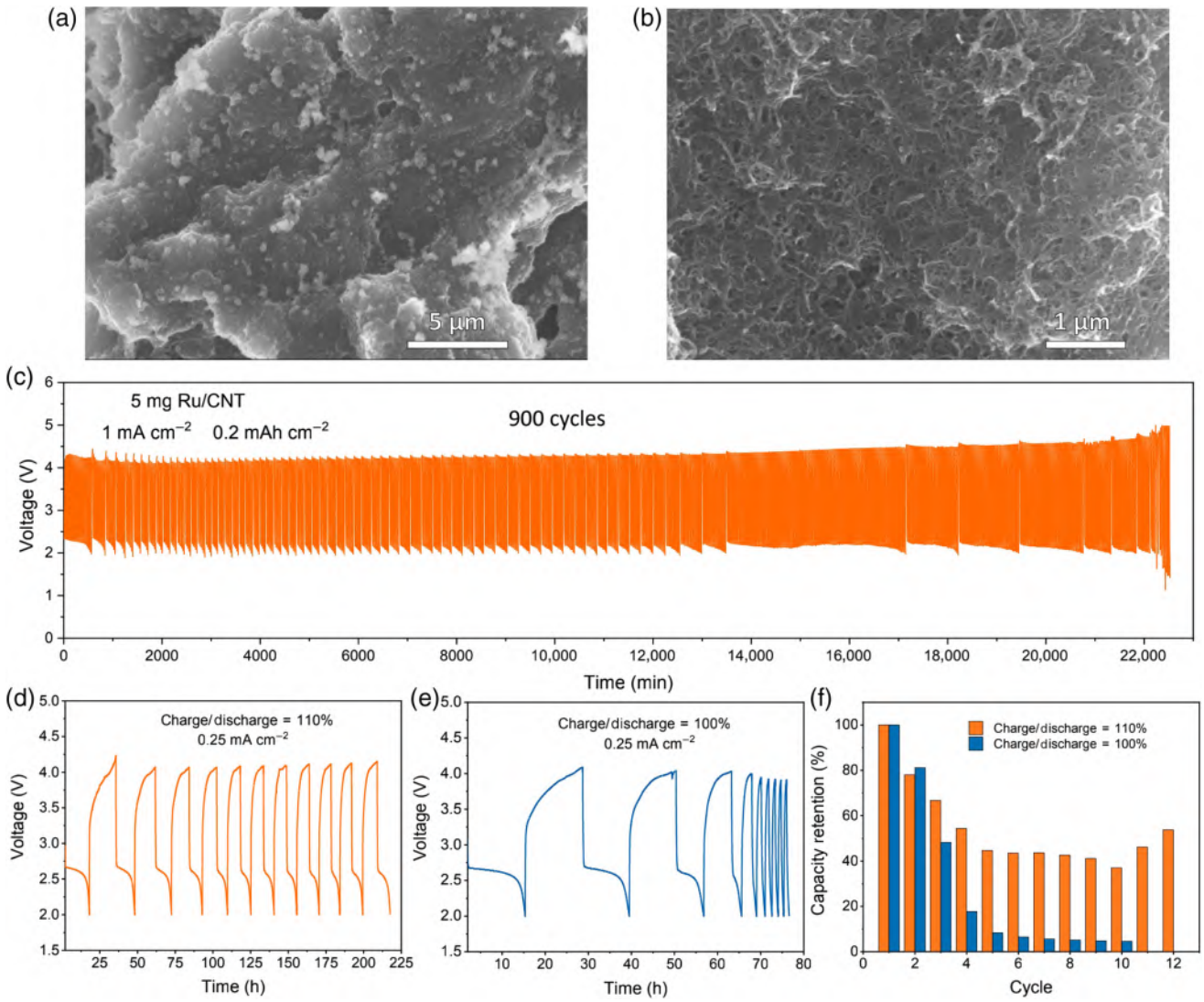

Figure 6 | *The performance of Li–O_2 batteries with high mass loading (5 mg Ru/CNT as the cathode). (a) Morphology of Ru/CNT cathode after battery failure. (b) Morphology of failed Ru/CNT cathode after overcharge. (c) Cycling performance of the Li–O_2 battery at a high rate of 1.0 mA cm^{-2} and 0.2 mAh cm^{-2}. Overcharge means that the charge capacity doubles the discharge capacity. (d and e) Full discharge-charge cycling performance of the Li–O_2 battery at 0.25 mA cm^{-2} with overcharge (charge/discharge = 110% capacity) and without overcharge (charge/discharge = 100% capacity). The initial capacities are higher than 3 mAh cm^{-2}. (f) Comparison of capacity retentions of batteries (d) with overcharge and (e) without overcharge.*

electrolyte (SSE). The role of the trace TEGDME and the Li^+ conduction mechanism in the SSE needs further investigation. We anticipated that the electrolyte could dry up before the final failure of the battery, and the electrolyte transformed to the SSE after decomposition to sustain longer battery life.

The above batteries were all based on CNT cathodes. To check whether overcharge would also be effective in ordinary carbon-based cathodes to improve battery performance, a Super P cathode was used as an example to configure a Li–O_2 battery. The battery only delivered a lifespan of 31 cycles in the traditional evaluation criterion, which could be extended to 98 cycles with the help of two times overcharge (Supporting Information Figure S16), proving that overcharge is a general method to regenerate the carbon-based cathodes. We anticipate that carbon-free cathodes could improve the performance further due to decreased side reactions.

Importantly, overcharge is not only effective in Li–O_2 batteries but also applicable in Na–O_2 and K–O_2 batteries. For the Na–O_2 battery, the first failure occurred after 73 cycles, and overcharging twice enabled the battery to work for 60 more cycles (Supporting Information Figure S17a). The thick solid electrolyte interphase (SEI) formed

DOI: 10.31635/ccschem.022.202201876
Citation: *CCS Chem.* **2023**, 5, 641–653
Link to VoR: https://doi.org/10.31635/ccschem.022.202201876

on the Na anode might be the reason for the large overpotential (Supporting Information Figure S17b). The K–O_2 battery was very unstable, with discharge voltage dropping to 2.0 V only after eight cycles. Since there are limited undecomposed products deposited on the cathode with this short life, the battery failure was presumably caused by the anode side. After overcharge, the battery revived with a much longer lifespan and higher overpotential, probably due to the overcharge-induced electrolyte decomposition that enabled the formation of a stable SEI on the K anode. In the following battery failure, the function of overcharge was to decompose the accumulated products on the cathode. Finally, the battery ran for 123 cycles, much longer than the initial nine cycles without overcharge (Supporting Information Figure S17c). After disassembling the battery, we found an even thicker SEI on the backside of the K anode (Supporting Information Figure S17d), resulting in a higher overpotential.

Conclusion

Our present work has identified that cathode passivation is the reason for the initial Li–O_2 battery failure and discussed the feasibility of extending the battery lifespan by overcharge. The discharge products and side products are not completely decomposed during the following fixed-capacity charge process due to the poor charge efficiency of the Li–O_2 battery; thus, a passivated layer forms on the cathode. As cycling goes on, this passivated layer continually accumulates and finally blocks the reaction sites and electron transfer pathways on the cathode, leading to the failure of the battery. After overcharge, the fatal passivated layer on the cathode can be removed to re-expose the active sites and rebuild the electron transfer pathways, reviving the failed Li–O_2 battery, and finally, extending the battery life from 180 to 1316 cycles. Besides, the battery life can be further prolonged by introducing CO_2 into the O_2 reaction gas to protect the Li anode, realizing system-level efficient use of each battery component; thus, a super-long life of 2714 cycles (more than 6300 h) could be achieved without changing the anode. We expect that if a better anode protection strategy is applied, a longer-life battery could be achieved, even though it is a very difficult approach. This overcharge strategy also works well on batteries with high-loading cathodes (5 mg cm^{-2} Ru/CNT) and high current densities (~900 cycles at 1 mA cm^{-2} and 0.2 mAh cm^{-2}).

The overcharge-induced battery revival strategy developed here can be further extended to Na– O_2 and K–O_2 batteries, which indicates that overcharge may be useful in other conversion-based batteries, like metal–CO_2 batteries and metal–SO_2 batteries. Traditional methods, including changing the failed cathode with a new one, typically involve tedious battery disassembly and re-assembly procedures, making battery recycling and regeneration an arduous task. Our results have shown an easier and safer metal–O_2 battery recycling strategy. Moreover, overcharge has long been conceived to be destructive to battery performance; this work has reshaped this impression and may inspire more considerations on the conceptual differences between LIBs and new emerging battery technologies.

Supporting Information

Supporting Information is available and includes additional experimental methods, SEM images, battery cycling performance, and characterization results.

Conflict of Interest

A Chinese patent has been granted no. ZL 2020 1 0312976.8. The authors declare no other competing interests.

Funding Information

This work was financially supported by the National Natural Science Foundation of China (21725103), National Key R&D Program of China (2020YFE0204500), Key Research Program of the Chinese Academy of Sciences (ZDRW-CN-2021-3), Changchun Science and Technology Development Plan Funding Project (21ZY06), and K. C. Wong Education Foundation (GJTD-2018-09).

Preprint Acknowledgement

The research presented in this article was posted on a preprint server before publication in CCS Chemistry. The corresponding preprint article can be found here: https://dx.doi.org/10.21203/rs.3.rs-823894/v1

References

1. McCloskey, B. D.; Speidel, A.; Scheffler, R.; Miller, D. C.; Viswanathan, V.; Hummelshoj, J. S.; Norskov, J. K.; Luntz, A. C. Twin Problems of Interfacial Carbonate Formation in Nonaqueous Li-O_2 Batteries. *J. Phys. Chem. Lett.* **2012**, *3*, 997–1001.

2. Mahne, N.; Schafzahl, B.; Leypold, C.; Leypold, M.; Grumm, S.; Leitgeb, A.; Strohmeier, G. A.; Wilkening, M.; Fontaine, O.; Kramer, D.; Slugovc, C.; Borisov, S. M.; Freunberger, S. A. Singlet Oxygen Generation as a Major Cause for Parasitic Reactions During Cycling of Aprotic Lithium-Oxygen Batteries. *Nat. Energy* **2017**, *2*, 17036.

3. Xu, J. J.; Wang, Z. L.; Xu, D.; Zhang, L. L.; Zhang, X. B. Tailoring Deposition and Morphology of Discharge Products

DOI: 10.31635/ccschem.022.202201876
Citation: *CCS Chem.* **2023**, 5, 641–653
Link to VoR: https://doi.org/10.31635/ccschem.022.202201876

towards High-Rate and Long-Life Lithium-Oxygen Batteries. *Nat. Commun.* **2013**, *4*, 2438.
4. Xu, J. J.; Xu, D.; Wang, Z. L.; Wang, H. G.; Zhang, L. L.; Zhang, X. B. Synthesis of Perovskite-Based Porous $La_{0.75}Sr_{0.25}MnO_3$ Nanotubes as a Highly Efficient Electrocatalyst for Rechargeable Lithium-Oxygen Batteries. *Angew. Chem. Int. Ed.* **2013**, *52*, 3887–3890.
5. Ottakam Thotiyl, M. M.; Freunberger, S. A.; Peng, Z.; Chen, Y.; Liu, Z.; Bruce, P. G. A Stable Cathode for the Aprotic Li-O_2 Battery. *Nat. Mater.* **2013**, *12*, 1050–1056.
6. Yu, Y.; Huang, G.; Du, J. Y.; Wang, J. Z.; Wang, Y.; Wu, Z. J.; Zhang, X. B. A Renaissance of N,N-Dimethylacetamide-Based Electrolyte to Promote the Cycling Stability of Li-O_2 Batteries. *Energy Environ. Sci.* **2020**, *13*, 3075–3081.
7. Yu, Y.; Zhang, X.-B. In Situ Coupling of Colloidal Silica and Li Salt Anion toward Stable Li Anode for Long-Cycle-Life Li-O_2 Batteries. *Matter* **2019**, *1*, 881–892.
8. Aetukuri, N. B.; McCloskey, B. D.; Garcia, J. M.; Krupp, L. E.; Viswanathan, V.; Luntz, A. C. Solvating Additives Drive Solution-Mediated Electrochemistry and Enhance Toroid Growth in Non-Aqueous Li-O_2 Batteries. *Nat. Chem.* **2015**, *7*, 50–56.
9. Jung, H. G.; Hassoun, J.; Park, J. B.; Sun, Y. K.; Scrosati, B. An Improved High-Performance Lithium-Air Battery. *Nat. Chem.* **2012**, *4*, 579–585.
10. Chen, Y.; Freunberger, S. A.; Peng, Z.; Fontaine, O.; Bruce, P. G. Charging a Li-O_2 Battery Using a Redox Mediator. *Nat. Chem.* **2013**, *5*, 489–494.
11. Gao, X.; Chen, Y.; Johnson, L.; Bruce, P. G. Promoting Solution Phase Discharge in Li-O_2 Batteries Containing Weakly Solvating Electrolyte Solutions. *Nat. Mater.* **2016**, *15*, 882–888.
12. Ma, J. L.; Meng, F. L.; Yu, Y.; Liu, D. P.; Yan, J. M.; Zhang, Y.; Zhang, X. B.; Jiang, Q. Prevention of Dendrite Growth and Volume Expansion to Give High-Performance Aprotic Bimetallic Li-Na Alloy-O_2 Batteries. *Nat. Chem.* **2019**, *11*, 64–70.
13. Lee, D. J.; Lee, H.; Kim, Y. J.; Park, J. K.; Kim, H. T. Sustainable Redox Mediation for Lithium-Oxygen Batteries by a Composite Protective Layer on the Lithium-Metal Anode. *Adv. Mater.* **2016**, *28*, 857–863.
14. Asadi, M.; Sayahpour, B.; Abbasi, P.; Ngo, A. T.; Karis, K.; Jokisaari, J. R.; Liu, C.; Narayanan, B.; Gerard, M.; Yasaei, P.; Hu, X.; Mukherjee, A.; Lau, K. C.; Assary, R. S.; Khalili-Araghi, F.; Klie, R. F.; Curtiss, L. A.; Salehi-Khojin, A. A Lithium–Oxygen Battery with a Long Cycle Life in an Air-Like Atmosphere. *Nature* **2018**, *555*, 502–506.
15. Xin, X.; Ito, K.; Dutta, A.; Kubo, Y. Dendrite-Free Epitaxial Growth of Lithium Metal During Charging in Li-O_2 Batteries. *Angew. Chem. Int. Ed.* **2018**, *57*, 13206–13210.
16. Zhang, X. P.; Sun, Y. Y.; Sun, Z.; Yang, C. S.; Zhang, T. Anode Interfacial Layer Formation via Reductive Ethyl Detaching of Organic Iodide in Lithium-Oxygen Batteries. *Nat. Commun.* **2019**, *10*, 3543.
17. Choudhury, S.; Wan, C. T. C.; Al Sadat, W. I.; Tu, Z. Y.; Lau, S.; Zachman, M. J.; Kourkoutis, L. F.; Archer, L. A. Designer Interphases for the Lithium-Oxygen Electrochemical Cell. *Sci. Adv.* **2017**, *3*, e1602809.
18. Liu, Q. C.; Xu, J. J.; Xu, D.; Zhang, X. B. Flexible Lithium-Oxygen Battery Based on a Recoverable Cathode. *Nat. Commun.* **2015**, *6*, 7892.
19. Dong, Q.; Li, T.; Yao, Y.; Wang, X.; He, S.; Li, J.; Luo, J.; Zhang, H.; Pei, Y.; Zheng, C.; Hong, M.; Qiao, H.; Gao, J.; Wang, D.; Yang, B.; Hu, L. A General Method for Regenerating Catalytic Electrodes. *Joule* **2020**, *4*, 2374–2386.
20. Ren, D.; Feng, X.; Lu, L.; He, X.; Ouyang, M. Overcharge Behaviors and Failure Mechanism of Lithium-Ion Batteries Under Different Test Conditions. *Appl. Energy* **2019**, *250*, 323–332.
21. Pushnitsa, K. A.; Kim, A. E.; Popovich, A. A.; Wang, Q.; Novikov, P. A. Structural Transformation of $LiNi_{0.8}Co_{0.1}Mn_{0.1}O_2$ Cathode Material During Cycling with Overcharge Investigated by in Situ X-Ray Diffraction. *J. Electron. Mater.* **2019**, *48*, 6694–6699.
22. Wu, L.; Nam, K.-W.; Wang, X.; Zhou, Y.; Zheng, J.-C.; Yang, X.-Q.; Zhu, Y. Structural Origin of Overcharge-Induced Thermal Instability of Ni-Containing Layered-Cathodes for High-Energy-Density Lithium Batteries. *Chem. Mater.* **2011**, *23*, 3953–3960.
23. Zhao, S.; Zhang, L.; Zhang, G.; Sun, H.; Yang, J.; Lu, S. Failure Analysis of Pouch-Type Li-O_2 Batteries with Superior Energy Density. *J. Energy Chem.* **2020**, *45*, 74–82.
24. Liu, T.; Feng, X. L.; Jin, X.; Shao, M. Z.; Su, Y. T.; Zhang, Y.; Zhang, X. B. Protecting the Lithium Metal Anode for a Safe Flexible Lithium-Air Battery in Ambient Air. *Angew. Chem. Int. Ed.* **2019**, *58*, 18240–18245.
25. Louli, A. J.; Eldesoky, A.; Weber, R.; Genovese, M.; Coon, M.; deGooyer, J.; Deng, Z.; White, R. T.; Lee, J.; Rodgers, T.; Petibon, R.; Hy, S.; Cheng, S. J. H.; Dahn, J. R. Diagnosing and Correcting Anode-Free Cell Failure via Electrolyte and Morphological Analysis. *Nat. Energy* **2020**, *5*, 693–702.
26. Xu, J. J.; Wang, Z. L.; Xu, D.; Meng, F. Z.; Zhang, X. B. 3D Ordered Macroporous $LaFeO_3$ as Efficient Electrocatalyst for Li-O_2 Batteries with Enhanced Rate Capability and Cyclic Performance. *Energy Environ. Sci.* **2014**, *7*, 2213–2219.
27. Chen, K.; Huang, G.; Ma, J. L.; Wang, J.; Yang, D. Y.; Yang, X. Y.; Yu, Y.; Zhang, X. B. The Stabilization Effect of CO_2 in Lithium-Oxygen/CO_2 Batteries. *Angew. Chem. Int. Ed.* **2020**, *59*, 16661–16667.

DOI: 10.31635/ccschem.022.202201876
Citation: *CCS Chem.* **2023**, 5, 641–653
Link to VoR: https://doi.org/10.31635/ccschem.022.202201876